Nonlinear Control of Multi-Quadrotor Flight Formations

Diogo Gomes Farinha dos Santos Ferreira
diogo.s.ferreira@tecnico.ulisboa.pt

Instituto Superior Técnico, Universidade de Lisboa, Portugal

December 2021

Abstract

The design of a control system based on modern control methods to control flight formations of multi-UAV quadrotors is presented. A leader-follower methodology is implemented where the leader has some predefined trajectory and a follower is controlled in order to track the leader keeping a constant displacement in its reference frame. The formation control system, responsible for the vehicle formation, considers, at first, only the motion at constant height, and secondly, the three-dimensional motion. In both cases, the nonlinear control laws are derived based on Lyapunov stability theory and the Backstepping method. The control laws are validated in simulation resorting to a realistic environment and vehicle models.

Keywords: Quadrotor, Flight Formation, Lyapunov Stability, Backstepping Method

1. Introduction

Unmanned Air Vehicles (UAVs), which were originally developed for military purposes, have now been devoted to a myriad of other uses, ranging from aerial photography, goods delivery, agriculture, mapping and surveillance, pollution monitoring or infrastructure inspections. When appropriately synchronized, a swarm of UAVs can perform much more complex tasks with gains in efficiency and robustness. As an example, [1] describes how it is possible to deploy two UAVs to cooperatively carry heavy loads. [2] presents a strategy for area exploration and mapping carried out by a swarm of autonomous UAVs. For policing and surveillance missions in areas where the communication range is limited, [3] discusses how efficient a network of UAVs can be in covering the area. For agriculture applications, [4] delves deeply into the advantages of using multiple UAVs with distributed control for better performance.

The examples mentioned apply different concepts of formation and control techniques. The control structure can be either centralized or decentralized. The centralized solutions rely on only one agent performing all computations and assigning the other agents their respective tasks, which makes them generally easier to design but more difficult to implement due to the heavy computational burden. The decentralized solutions break down the computational burden into smaller problems to be solved by all the agents, so they are more intricate to design but their implementation is more reliable and robust.

The most relevant formation control concepts are the leader-follower, the virtual leader and the behavior-based. In the leader-follower case, a formation is achieved when each follower drives into the desired position with respect to the leader, which has some known trajectory. In the second case, the virtual leader describes a reference trajectory and the formation is achieved when all the vehicles in the swarm follow the leader in a rigid structure. The behavior-based formation control approach defines different control behaviors for different situations of interest, as explained by [5].

This work will focus on implementing a leader-follower strategy where a follower is intended to chase a leader keeping a constant displacement.

2. Quadrotor Model

Let $\{I\}$ be an orthonormal reference frame according to the North-East-Down (NED) coordinate system. Let $\{B\}$ be another orthonormal reference frame centred at point p. The orientation of $\{B\}$ with respect to $\{I\}$ is given by the Euler angles $\lambda = (\phi, \theta, \psi)$ that represent the rotation about their respective axes. The rotation matrix from $\{B\}$ to $\{I\}$ is given by an orthogonal matrix

$$R \in SO\left(3\right) \triangleq \{X \in \mathbb{R}^{3\times 3} : XX^T = X^T X = \mathbf{I}_3, |X| = 1\}. \tag{1}$$

From the definition of R, its derivative is $\dot{R} = RS\left(\omega\right)$, with ω the angular velocity of $\{B\}$ expressed in $\{B\}$. Let p be the quadrotor's position, v its velocity, m its mass and J its inertia tensor.

Let also f be the sum of external forces applied on the quadrotor expressed in $\{I\}$ and n the sum of external moments expressed in $\{B\}$. For any $\theta \neq (2k+1)\frac{\pi}{2} \quad \forall\, k \in \mathbb{Z}$, the complete dynamics of the quadrotor is given by

$$\begin{cases} \dot{p} = v \\ m\dot{v} = f \\ J\dot{\omega} = -S(\omega) J\omega + n \\ \dot{R} = RS(\omega) \end{cases}, \tag{2}$$

where $S(\omega)$ is a skew-symmetric matrix such that $S(x)\, y = x \times y$ for any $x, y \in \mathbb{R}^3$.

3. 2D Formation Control

A trajectory tracking controller is implemented to make the follower track the leader while keeping a constant offset in its reference frame. Assuming the movement at constant height, equation (2) can be simplified for a purely kinematic model given by

$$\begin{cases} \dot{x} = u\cos\psi - v\sin\psi \\ \dot{y} = u\sin\psi + v\cos\psi \\ \dot{\psi} = r \end{cases}. \tag{3}$$

If $\Delta = (\Delta_x, \Delta_y)^T$ is the desired displacement, R the 2D rotation matrix, $p, c \in \mathbb{R}^2$ the follower's and leader's positions, respectively, the position error can be written as

$$z_1 = R^T(c-p) - \Delta \tag{4}$$

and its derivative as

$$\dot{z}_1 = R^T\dot{c} - v - S(r)(z_1 + \Delta). \tag{5}$$

Consider a Lyapunov function $V_1 = \frac{1}{2}\|z_1\|^2$. Its derivative is

$$\dot{V}_1 = z_1^T\left(R^T\dot{c} - v - S(r)\Delta\right). \tag{6}$$

Adding and subtracting a term $k_1\|z_1\|^2$ yields

$$\dot{V}_1 = k_1\|z1\|^2 + z_1^T z_2 \tag{7}$$

where a new error $z_2 = k_1 z_1 + R^T\dot{c} - v - S(r)\Delta$ was introduced. Let now $V_2 = V_1 + \frac{1}{2}\|z_2\|^2$ be an augmented Lyapunov function. Its derivative is

$$\dot{V}_2 = \dot{V}_1 + z_2^T\Big[k_1\dot{z}_1 + R^T\ddot{c} - S(r)R^T\dot{c} - \begin{pmatrix} 1 & -\Delta_y \\ 0 & \Delta_x \end{pmatrix}\begin{pmatrix} \dot{v} \\ \dot{r} \end{pmatrix}\Big]. \tag{8}$$

If the accelerations $\dot{v}$, $\dot{r}$ are considered inputs of the system, the control law should be

$$\begin{pmatrix} \dot{v} \\ \dot{r} \end{pmatrix} = \begin{pmatrix} 1 & -\Delta_y \\ 0 & \Delta_x \end{pmatrix}^{-1}\left(k_1\dot{z}_1 + R^T\ddot{c} - S(r)R^T\dot{c} + z_1 + k_2 z_2\right), \tag{9}$$

which is well-defined for $\Delta_x \neq 0$. Under this control law, the error system can be written in strict-feedback form [6] as

$$\begin{cases} \dot{z}_1 = -\left(S(r) + k_1 I_2\right) z_1 + z_2 \\ \dot{z}_2 = -z_1 - k_2 z_2 \end{cases} \tag{10}$$

and the derivative of V_2 becomes

$$\dot{V}_2 = -k_1\|z_1\|^2 - k_2\|z_2\|^2, \tag{11}$$

which is negative for $(z_1, z_2) \neq 0$ if $k_1, k_2 > 0$. Thus, according to the Barbashin-Krasovskii theorem [6, theorem 4.2], the error system is globally asymptotically stable around the origin.

3.1. Perturbed system

Consider the existence of an unknown external disturbance d such that

$$\dot{z}_2 = k_1\dot{z}_1 + R^T\ddot{c} - S(r)R^T\dot{c} - \dot{v} - S(\dot{r})\Delta + Rd. \tag{12}$$

Additionally, assume the controller is equipped with a disturbance estimator $\hat{d}$ such that

$$\begin{pmatrix} \dot{v} \\ \dot{r} \end{pmatrix} = \begin{pmatrix} 1 & -\Delta_y \\ 0 & \Delta_x \end{pmatrix}^{-1}\Big(k_1\dot{z}_1 + R^T\ddot{c} - S(r)R^T\dot{c} + z_1 + k_2 z_2 + R\hat{d}\Big). \tag{13}$$

Considering the estimation error $\tilde{d} = d - \hat{d}$ as an input to the error system with state $z = (z_1, z_2)^T$, the error dynamics can be written in state space as

$$\dot{z} = \underbrace{\begin{pmatrix} -(S(r) + k_1 I_2) & I_2 \\ -I_2 & -k_2 I_2 \end{pmatrix}}_{\text{A}} z + \underbrace{\begin{pmatrix} 0_2 \\ R \end{pmatrix}}_{\text{B}} \tilde{d}, \tag{14}$$

where 0_2 is the null matrix of size 2×2. Now, we wish to design an adaptive controller for the estimator $\hat{d}$. Let $V_3 : \mathbb{R}^6 \to \mathbb{R}$ be a continuously differentiable Lyapunov function such that $V_3(0) = 0$, $V_3(z, \tilde{d}) > 0, \forall (z, \tilde{d}) \neq 0$ and $\|(z, \tilde{d})\| \to \infty \Rightarrow V_3(z, \tilde{d}) \to \infty$ given by $V_3 = V_2 + \frac{1}{2k_d}\|\tilde{d}\|^2$. Its derivative is computed as

$$\dot{V}_3 = z^T A z + z^T B\tilde{d} + \frac{1}{k_d}\tilde{d}^T\dot{\tilde{d}}. \tag{15}$$

The first term of $\dot{V}_3$ is negative for all $\mathbf{z} \neq 0$ as it has already been proved the error system converges under the control law from equation (9). As of the remaining two terms, $\dot{V}_3$ gets negative for all $(z, \tilde{d}) \neq 0$ if they sum to zero. So,

$$\dot{\tilde{d}}^T = -k_d z^T B. \tag{16}$$

If the disturbance is assumed constant, then $\dot{\tilde{d}} = -\dot{\hat{d}}$, so the adaptation law for the estimator is

$$\dot{\hat{d}} = k_d \begin{pmatrix} 0_2 & R \end{pmatrix} z. \tag{17}$$

Now that we have the tracking control and the disturbance estimation, we must study the stability of the system comprised of both the position error and the disturbance estimation error simultaneously. This system is given by

$$\begin{pmatrix} \dot{z} \\ \dot{\tilde{d}} \end{pmatrix} = \begin{pmatrix} A & B \\ -k_d B^T & 0_2 \end{pmatrix} \begin{pmatrix} z \\ \tilde{d} \end{pmatrix}. \tag{18}$$

Let $\Omega = \{(z, \tilde{d}) \in \mathbb{R}^6 : V_3(z, \tilde{d}) \leq c\}$ for any $c \in \mathbb{R}^+$. The set Ω is compact since V_3 is radially unbounded and, from Lyapunov's direct method [6, theorem 4.1], it is positively invariant with respect to the dynamics (18). Let E be the set of all points in Ω where $\dot{V}_3(z, \tilde{d}) = 0$. This set is given by

$$E = \{(z, \tilde{d}) \in \mathbb{R}^6 : z = 0\}. \tag{19}$$

Let M be the largest invariant set contained in E. By LaSalle's theorem [6, theorem 4.4], every solution with initial condition in Ω approaches M as $t \to \infty$. Since for any $(z, \tilde{d}) \in \mathbb{R}^6$ there exists a $c > 0$ such that $(z, \tilde{d}) \in \Omega$, we have that any solution converges to M. From its invariance and recalling system (14), we have that, for all $(z, \tilde{d}) \in M$,

$$\begin{aligned} \dot{z} = 0 \;&\Leftrightarrow\; B\tilde{d} = 0_{4\times 1} \\ &\Leftrightarrow\; \tilde{d} = 0_{2\times 1}. \end{aligned} \tag{20}$$

Therefore, $(z, \tilde{d}) = 0$ is the only element in M and the system is globally asymptotically stable around the origin.

3.2. Closed-loop system

After deriving a control law, it is of interest to study the stability of the closed-loop system, i.e., the formation of one leader and one follower. When the position error is identically zero, $z_1 = \dot{z}_1 = 0$ and equation (5) becomes

$$R^T \dot{c} - v - S(r)\,\Delta = 0. \tag{21}$$

Assuming a general leader's trajectory $\dot{c} = C\begin{pmatrix}\cos\psi_c & \sin\psi_c\end{pmatrix}^T$, the closed-loop equation can be expanded to isolate the control variables as

$$\begin{pmatrix} v \\ r \end{pmatrix} = \begin{pmatrix} C\cos(\psi - \psi_c) - \frac{C\Delta_y}{\Delta_x}\sin(\psi - \psi_c) \\ -\frac{C}{\Delta_x}\sin(\psi - \psi_c) \end{pmatrix}, \tag{22}$$

well defined for $\forall \Delta_x \neq 0$. These equations describe a nonlinear periodic system with a dynamics for ψ and output v. The equilibrium points of the system from equation (22) are

$$\psi^* = \psi_c + k\pi \quad, \forall k \in \mathbb{Z}. \tag{23}$$

To analyse stability, one can consider infinitesimal disturbances around these equilibrium points. Let $\psi = \psi_c + 2k\pi + \epsilon \quad, \epsilon > 0$. Then, system (22) becomes

$$\begin{aligned} \dot{\psi} &= -\frac{C}{\Delta_x}\sin(2k\pi + \epsilon) \\ &\approx -\frac{C}{\Delta_x}\epsilon, \end{aligned} \tag{24}$$

which is negative if $\Delta_x > 0$. Thus, the system is asymptotically stable in the vicinity $\epsilon > 0$ of the equilibrium points $\psi^* = \psi_c + 2k\pi \quad, \forall k \in \mathbb{Z}$. Similarly, we can conclude it is unstable in the vicinity $\epsilon > 0$ of the equilibrium points $\psi^* = \psi_c + (2k+1)\pi \quad, \forall k \in \mathbb{Z}$. A phase portrait of the system when $\psi_c = 0$ is represented in figure 1. It is easy to see that the region of convergence of the equilibrium point $\psi^* = \psi_c + 2k\pi$ is

$$\psi \in \,]\psi_c + (2k-1)\pi; \psi_c + (2k+1)\pi[\quad, \forall k \in \mathbb{Z}. \tag{25}$$

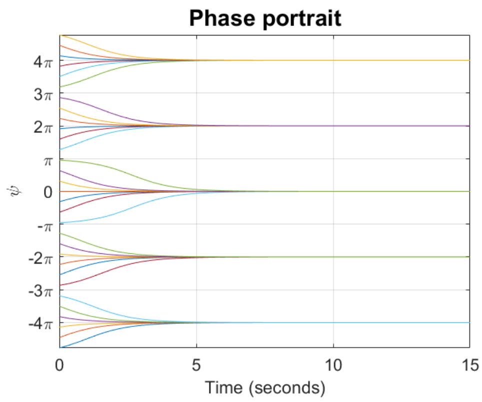

Figure 1: Phase portrait of the system $\dot{\psi} = -\sin(\psi)$.

In conclusion, the follower can have a heading difference relative to the leader of up to 180°. The bigger the difference, the slower is the convergence to the desired heading. In the limit, if a follower is set to track a leader describing a linear path, starting in opposite heading, it will not converge.

4. 3D Formation Control

The motion of the quadrotor at constant height has been studied and a controller for the simplified model has been derived using the backstepping method applied to the position error. This method is now used to derive a similar nonlinear controller for the complete model. The dynamics from equation (2) can be written in a state-space form by introducing the state vector $X = \left(\phi, \dot{\phi}, \theta, \dot{\theta}, \psi, \dot{\psi}, z, \dot{z}, x, \dot{x}, y, \dot{y}\right)^T$ and the input vector $U = (T, n_x, n_y, n_z)^T$, according to [7], as

$$f(X,U) = \begin{cases} \dot{\phi} \\ a_\phi \dot{\theta}\dot{\psi} \\ \dot{\theta} \\ a_\theta \dot{\phi}\dot{\psi} + b_\theta n_y \\ \dot{\psi} \\ a_\psi \dot{\phi}\dot{\theta} + b_\psi n_z \\ \dot{z} \\ g - \frac{T}{m}\cos\phi\cos\theta \\ \dot{x} \\ \frac{T}{m} u_x \\ \dot{y} \\ \frac{T}{m} u_y \end{cases}, \quad (26)$$

with the definitions

$$\begin{aligned} u_x &= \cos\phi\sin\theta\cos\psi + \sin\phi\sin\psi; \\ u_y &= \cos\phi\sin\theta\sin\psi - \sin\phi\cos\psi \end{aligned} \quad (27)$$

and the constants

$$\begin{aligned} a_\phi &= \frac{J_y - J_z}{J_x}; \quad a_\theta = \frac{J_z - J_x}{J_y}; \quad a_\psi = \frac{J_x - J_y}{J_z}; \\ b_\phi &= \frac{1}{J_x}; \quad b_\theta = \frac{1}{J_y}; \quad b_\psi = \frac{1}{J_z}. \end{aligned} \quad (28)$$

The system as it is posed highlights an important relation between the position and attitude of the quadrotor: the position components depend on the angles, however the opposite is not true. The overall system can be thought of as the result of two semi-decoupled subsystems: the translation and the rotation – for which two controllers are designed separately.

4.1. Attitude Control

Let $z_\phi = \phi_{ref} - \phi$ be the roll angle error. Let $V_\phi = \frac{1}{2}z_\phi^2$ be a Lyapunov function with derivative

$$\dot{V}_\phi = z_\phi\left(\dot{\phi}_{ref} - \dot{\phi}\right) \quad (29)$$

If $\dot{\phi}$ is controlled to be

$$\dot{\phi} = \dot{\phi}_{ref} + k_\phi z_\phi, \quad (30)$$

then $\dot{V}_\phi = -k_\phi z_\phi^2$. Let now $z_{\dot{\phi}}$ be the roll rate error given by

$$z_{\dot{\phi}} = \dot{\phi} - \dot{\phi}_{ref} - k_\phi z_\phi \quad (31)$$

and the augmented Lyapunov function

$$V_{\dot{\phi}} = V_\phi + \frac{1}{2}z_{\dot{\phi}}^2 \quad (32)$$

with its derivative given by

$$\dot{V}_{\dot{\phi}} = -k_\phi z_\phi^2 + z_{\dot{\phi}}\left(a_\phi\dot{\theta}\dot{\psi} + b_\phi n_x - \ddot{\phi}_{ref} - k_\phi \dot{z}_\phi\right). \quad (33)$$

If the control law for n_x is chosen to be

$$n_x = \frac{1}{b_\phi}\left(\ddot{\phi}_{ref} + k_\phi \dot{z}_\phi - a_\phi\dot{\theta}\dot{\psi} - k_{\dot{\phi}} z_{\dot{\phi}}\right) \quad (34)$$

then

$$\dot{V}_{\dot{\phi}} = -k_\phi z_\phi^2 - k_{\dot{\phi}} z_{\dot{\phi}}^2 \quad (35)$$

which is negative for $(z_\phi, z_{\dot{\phi}}) \neq 0$ if $k_\phi, k_{\dot{\phi}} > 0$. Thus, according to the Barbashin-Krasovskii theorem [6, theorem 4.2], the roll error system is globally asymptotically stable around the origin. Following the same backstepping procedure for the remaining angular variables, an attitude controller is derived as

$$\begin{cases} n_x = \frac{1}{b_\phi}\Big(\ddot{\phi}_{\rm ref} + k_\phi(\dot{\phi}_{\rm ref} - \dot{\phi}) - a_\phi\dot{\theta}\dot{\psi} \\ \qquad - k_{\dot{\phi}}[\dot{\phi} - \dot{\phi}_{\rm ref} - k_\phi(\phi_{\rm ref} - \phi)]\Big) \\ n_y = \frac{1}{b_\theta}\Big(\ddot{\theta}_{\rm ref} + k_\theta(\dot{\theta}_{\rm ref} - \dot{\theta}) - a_\theta\dot{\phi}\dot{\psi} \\ \qquad - k_{\dot{\theta}}[\dot{\theta} - \dot{\theta}_{\rm ref} - k_\theta(\theta_{\rm ref} - \theta)]\Big) \\ n_z = \frac{1}{b_\psi}\Big(\ddot{\psi}_{\rm ref} + k_\psi(\dot{\psi}_{\rm ref} - \dot{\psi}) - a_\psi\dot{\phi}\dot{\theta} \\ \qquad - k_{\dot{\psi}}[\dot{\psi} - \dot{\psi}_{\rm ref} - k_\psi(\psi_{\rm ref} - \psi)]\Big) \end{cases}, \quad (36)$$

with gains $k_\phi, k_{\dot{\phi}}, k_\theta, k_{\dot{\theta}}, k_\psi, k_{\dot{\psi}} > 0$.

4.2. Position Control

Let $z_z = z_{ref} - z$ be the altitude error. Let $V_\phi = \frac{1}{2}z_z^2$ be a Lyapunov function with derivative

$$\dot{V}_z = z_z\left(\dot{z}_{ref} - \dot{z}\right). \quad (37)$$

If $\dot{z}$ is controlled to be

$$\dot{z} = \dot{z}_{ref} + k_z z_z, \quad (38)$$

then $\dot{V}_z = -k_z z_z^2$. Let now $z_{\dot{z}}$ be the vertical speed error given by

$$z_{\dot{z}} = \dot{z} - \dot{z}_{ref} - k_z z_z \quad (39)$$

and the augmented Lyapunov function

$$V_{\dot{z}} = V_z + 1/2 z_{\dot{z}}^2 \quad (40)$$

with its derivative given by

$$\dot{V}_{\dot{z}} = -k_z z_z^2 + z_{\dot{z}}\left(g - \frac{T}{m}\cos\phi\cos\theta - \ddot{z}_{ref} - k_z \dot{z}_z\right). \quad (41)$$

If the control law for T is chosen to be

$$T = \frac{m}{\cos\phi\cos\theta}(g - \ddot{z}_{ref} - k_z\dot{z}_z - k_{\dot{z}} z_{\dot{z}}), \quad (42)$$

then

$$\dot{V}_{\dot{z}} = -k_z z_z^2 - k_{\dot{z}} z_{\dot{z}}^2 \quad (43)$$

which is negative for $(z_z, z_{\dot{z}}) \neq 0$ if $k_z, k_{\dot{z}} > 0$. Thus, according to the Barbashin-Krasovskii theorem [6, theorem 4.2], the altitude error system is globally asymptotically stable around the origin. Following the same backstepping procedure for the remaining position variables, a position controller is derived as

$$\begin{cases} T = \dfrac{m}{\cos\phi\cos\theta}\left(g - \ddot{z}_{\text{ref}} - k_z(\dot{z}_{\text{ref}} - \dot{z})\right. \\ \qquad\qquad \left. -k_{\dot{z}}[\dot{z} - \dot{z}_{\text{ref}} - k_z(z_{\text{ref}} - z)]\right) \\ u_x = \dfrac{m}{T}\left(\ddot{x}_{\text{ref}} + k_x(\dot{x}_{\text{ref}} - \dot{x}) - k_{\dot{x}}[\dot{x} - \dot{x}_{\text{ref}}\right. \\ \qquad\qquad \left. -k_x(x_{\text{ref}} - x)]\right) \\ u_y = \dfrac{m}{T}\left(\ddot{y}_{\text{ref}} + k_y(\dot{y}_{\text{ref}} - \dot{y}) - k_{\dot{y}}[\dot{y} - \dot{y}_{\text{ref}}\right. \\ \qquad\qquad \left. -k_y(y_{\text{ref}} - y)]\right) \end{cases} . \tag{44}$$

with gains $k_x, k_{\dot{x}}, k_y, k_{\dot{y}}, k_z, k_{\dot{z}} > 0$.

In order to feed the attitude controller with the reference values for roll and pitch, the definitions (27) are recalled and written in the following format:

$$\begin{pmatrix} u_x \\ u_y \end{pmatrix} = \begin{pmatrix} \cos\psi & \sin\psi \\ \sin\psi & -\cos\psi \end{pmatrix} \begin{pmatrix} A \\ B \end{pmatrix}, \tag{45}$$

where A and B are auxiliary variables defined as

$$A = \cos\phi\sin\theta; \quad B = \sin\phi. \tag{46}$$

This system is always invertible for any ψ although it is highly nonlinear and multiple solutions are possible. To avoid any singularities and reduce the computational burden of these calculations, a simplified system is considered under the assumption that the quadrotor does not perform complex manoeuvres thereby keeping the roll and pitch angles small enough. In this case, $A \approx \theta$ and $B \approx \phi$ and the inputs of the attitude controller are

$$\begin{pmatrix} \theta_{\text{ref}} \\ \phi_{\text{ref}} \end{pmatrix} = \begin{pmatrix} \cos\psi & \sin\psi \\ \sin\psi & -\cos\psi \end{pmatrix} \begin{pmatrix} u_x \\ u_y \end{pmatrix}. \tag{47}$$

The attitude controller also requires the derivative and second derivative of the reference Euler angles. These derivatives could be explicitly computed from systems (45) or (47), however that would require measurements of the acceleration and its derivative, which are in all likelihood unavailable. A numerical differentiation of the reference angles is suggested by [8] and adapted to

$$\dot{\phi}_{\text{ref}} \approx \frac{\phi_{\text{ref}}(t) - \phi_{\text{ref}}(t - \Delta t)}{\Delta t}, \tag{48}$$

$$\dot{\theta}_{\text{ref}} \approx \frac{\theta_{\text{ref}}(t) - \theta_{\text{ref}}(t - \Delta t)}{\Delta t}, \tag{49}$$

where Δt is the sampling period. The second derivative of the reference angles can be computed likewise. The controller scheme is shown in figure 2.

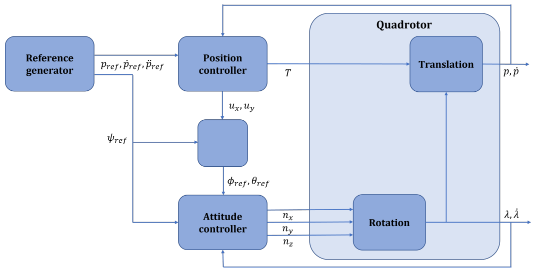

Figure 2: 3D controller scheme.

5. Simulation results

Several simulations have been carried out for the developed architectures. This section presents an illustrative simulation for both the 2D and 3D controllers, where the physical parameters are shown in SI units.

5.1. 2D simulation

The simulation consists of a follower tracking a leader in a circular path. The displacement is $\Delta = (1, 1)$, the disturbance intensity is $d = (1, 1)$ and the gains are shown in table 1. Figure 3 shows the simulation output where the follower converges to a trajectory where it sees the leader at position $(1, 1)$ in its reference frame.

2D controller gains	
k_1	0.5 s^{-1}
k_2	0.5 s^{-1}
k_d	0.5

Table 1: 2D controller gains.

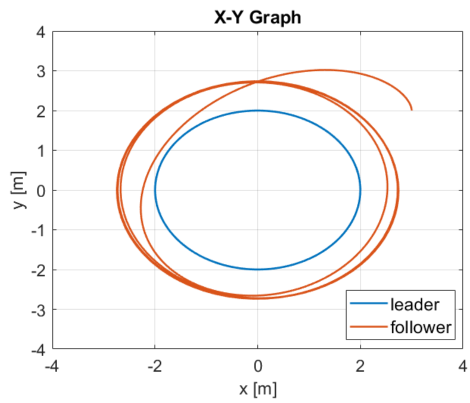

Figure 3: 2D simulation: position plot.

5.2. 3D simulation

For the 3D case, a complete model simulation simulation is done for a formation of one leader and two followers, each of them with equal controllers as defined in table 2 and departing from the same place. The heavy quadrotor model developed by [9] was used. The first follower keeps a displacement of $\Delta_1 = (1, 1, 0)$ m and the second followers keeps a displacement of $\Delta_2 = (2, 2, 0)$. To add a little more reality into the simulation, white Gaussian noise is added to the sensors of the followers with signal-to-noise ratio equal to 45 dB. The simulation results are represented in figures 4 to 9, including state variables, displacement to the leader and actuation.

Attitude			
k_ϕ	$1\ \mathrm{s}^{-1}$	$k_{\dot{\phi}}$	$1\ \mathrm{s}^{-1}$
k_θ	$1\ \mathrm{s}^{-1}$	$k_{\dot{\theta}}$	$1\ \mathrm{s}^{-1}$
k_ψ	$1\ \mathrm{s}^{-1}$	$k_{\dot{\psi}}$	$1\ \mathrm{s}^{-1}$
Position			
k_x	$2.2\ \mathrm{s}^{-1}$	$k_{\dot{x}}$	$0.18\ \mathrm{s}^{-1}$
k_y	$2.2\ \mathrm{s}^{-1}$	$k_{\dot{y}}$	$0.18\ \mathrm{s}^{-1}$
k_z	$0.5\ \mathrm{s}^{-1}$	$k_{\dot{z}}$	$0.2\ \mathrm{s}^{-1}$

Table 2: Controller gains for 3D circular tracking.

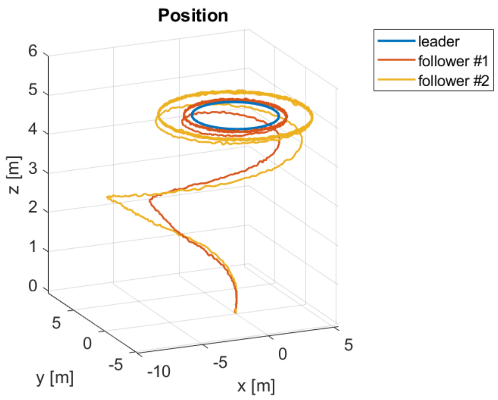

Figure 4: 3D simulation: position plot.

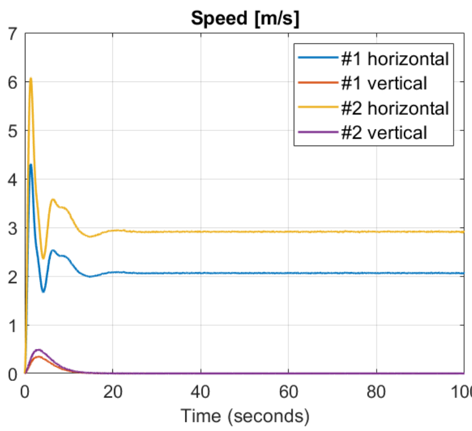

Figure 5: 3D simulation: speed plot.

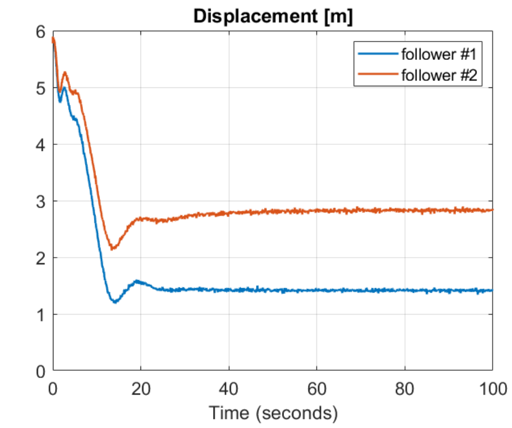

Figure 6: 3D simulation: displacement plot.

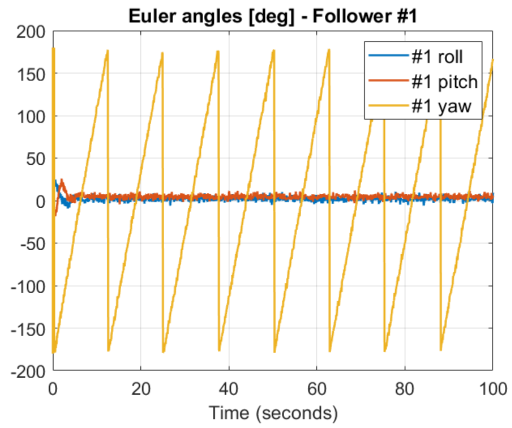

Figure 7: 3D simulation: Euler angles plot for follower 1.

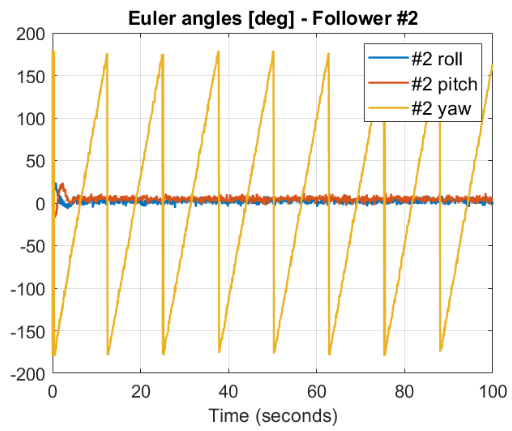

Figure 8: 3D simulation: Euler angles plot for follower 2.

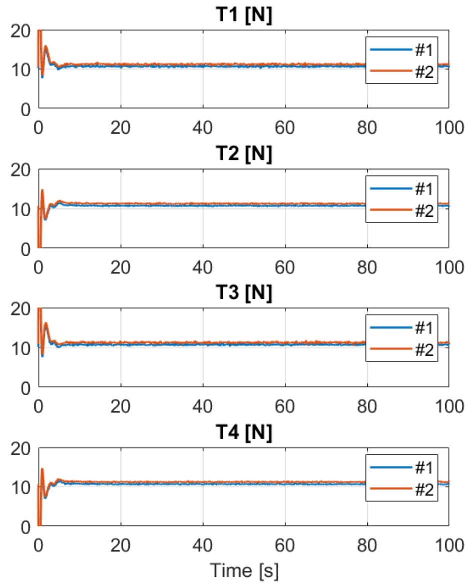

Figure 9: 3D simulation: required thrust.

6. Conclusions

This work proposes an approach to the formation control of quadrotors by solving the trajectory tracking problem using nonlinear control. The controller is applied to a leader-follower formation based on the backstepping method. The 2D controller is kinematic but robust to constant acceleration disturbances and the formation stability is guaranteed. As far as the 3D motion is concerned, a controller has been developed for a kinematic and dynamic model and the control laws have been proved stable.

In this work it is assumed all variables of interest are known by the follower. One topic for future work can be the estimation of variables unknown to some vehicles in a larger formation. Another suggestion of future work can include incorporating collision avoidance techniques and adapting the formation framework to dodge uninvited obstacles.

References

[1] T. Bacelar, C. Cardeira, and P. Oliveira, "Cooperative load transportation with quadrotors," in *2019 IEEE International Conference on Autonomous Robot Systems and Competitions (ICARSC)*, 2019, pp. 1–6. DOI: 10.1109/ICARSC.2019.8733619.

[2] M. Rosalie, J. E. Dentler, G. Danoy, P. Bouvry, S. Kannan, M. A. Olivares-Mendez, and H. Voos, "Area exploration with a swarm of uavs combining deterministic chaotic ant colony mobility with position mpc," in *2017 International Conference on Unmanned Aircraft Systems (ICUAS)*, 2017, pp. 1392–1397. DOI: 10.1109/ICUAS.2017.7991418.

[3] J. Scherer and B. Rinner, "Multi-uav surveillance with minimum information idleness and latency constraints," *IEEE Robotics and Automation Letters*, vol. 5, no. 3, pp. 4812–4819, 2020. DOI: 10.1109/LRA.2020.3003884.

[4] C. Ju and H. I. Son, "Multiple uav systems for agricultural applications: Control, implementation, and evaluation," *Electronics*, vol. 7, no. 9, 2018, ISSN: 2079-9292. DOI: 10.3390/electronics7090162.

[5] T. Balch and R. Arkin, "Behavior-based formation control for multirobot teams," *IEEE Transactions on Robotics and Automation*, vol. 14, no. 6, pp. 926–939, 1998. DOI: 10.1109/70.736776.

[6] H. K. Khalil, *Nonlinear Systems*, 3rd edition. Pearson, 2014.

[7] S. Bouabdallah and R. Siegwart, "Backstepping and sliding-mode techniques applied to an indoor micro quadrotor," in *Proceedings of the 2005 IEEE International Conference on Robotics and Automation*, 2005, pp. 2247–2252. DOI: 10.1109/ROBOT.2005.1570447.

[8] R. Pérez-Alcocer, J. Moreno-Valenzuela, and R. Miranda-Colorado, "A robust approach for trajectory tracking control of a quadrotor with experimental validation," *ISA Transactions*, vol. 65, pp. 262–274, 2016, ISSN: 0019-0578. DOI: https://doi.org/10.1016/j.isatra.2016.08.001.

[9] P. Pounds, R. Mahony, and P. Corke, "Modelling and control of a large quadrotor robot," *Control Engineering Practice*, vol. 18, no. 7, pp. 691–699, 2010, Special Issue on Aerial Robotics, ISSN: 0967-0661. DOI: https://doi.org/10.1016/j.conengprac.2010.02.008.